Publication P4

Jere Kolehmainen. 2010. Optimal dovetail permanent magnet rotor solutions for various pole numbers. IEEE Transactions on Industrial Electronics, volume 57, number 1, pages 70-77.

Optimal Dovetail Permanent Magnet Rotor Solutions for Various Pole Numbers

Jere Kolehmainen

***Abstract*—A buried magnet rotor structure, which is supported only by permanent magnets, is proposed for medium-speed permanent magnet machines. Many design aspects of the dovetail-shaped rotor structure have been found. Various machine solutions, with pole numbers 6 to 14, are studied with electromagnetic and structural finite element simulations. A simple model is created for making comparison with the different pole numbers easier. Main dimensions of the machine are kept the same. Optimal solutions for various pole numbers are searched and discussed. It is shown that for lower pole numbers, the structure is electrically better, while for higher pole numbers, the structure is mechanically stronger against centrifugal forces. In addition, the optimal electromagnetic structures for each pole number are shown to be similar to the optimal mechanical structures. Electrically and mechanically critical areas are also shown to be almost the same. The optimized results are also compared to three manufactured prototypes. The obtained results demonstrate the feasibility of the construction and the design method.**

***Index Terms*—Design methodology, electromagnetic analysis, optimization methods, permanent magnet machines, rotating machine mechanical factors, structural engineering, synchronous machines.**

I. Introduction

PERMANENT magnet synchronous machines with buried magnets have been considered in a wide range of variable speed drives [1]. A buried magnet design has many advantages compared to the designs with the surface mounted and the inset magnets [2], [3]. With the buried magnet design, the flux concentration can be achieved, which induces the higher air-gap flux density [4], [5]. That, in turn, gives a possibility to increase torque of a machine. In addition, the buried magnets have better protection against demagnetization and eddy currents because they are further from the air gap [4]. Therefore, the rotor solutions with the buried magnets are also a good choice for high speed and frequency machines [6]. With high rotational speeds, mechanical stability of the rotor often arises to a problem to solve. However, stability of whole drive systems can be increased by using right control strategies [1], [7], [8].

The typical way of manufacturing a buried permanent magnet rotor is to assemble a stack of punched and solid rotor disks with rectangular holes and insert magnets into these holes [1]–[6]. Rotor disks can also be punched to many pieces, when extra supporting structure is needed. For example, the typical supporting method for V-shaped buried magnet pole structures is to support separate rotor poles with H-shaped bars in the bottoms of the V-shaped poles. However, solutions with solid rotor sheets, where the rotor poles between the magnets are fixed to the rest of the rotor structure with thin iron bridges, are easier to manufacture. The disadvantage of the supporting bridges is the leakage flux, the magnitude of which depends on the thickness of the bridges. In low-speed applications, this is not a problem, since the centrifugal forces acting on the poles are relatively small and the bridges can be kept thin. However, as the tangential speed of the rotor surface exceeds 60 m/s (corresponding to 4000 1/min in machine size IEC250), the stress in the bridges will exceed the yield strength of the electrical steel (typically 300 MPa for grade M400-50A). With solid rotor sheet solution, the problem can be countered by increasing the thickness of the bridges [5], [6]. However, thicker iron bridges increase the leakage flux, which, in turn, increases the amount of magnet material needed to get the required torque.

Stronger bridges constitute larger routes for the leakage flux. This contradiction between mechanical and electrical designs is studied earlier for a high-speed interior permanent magnet machine rotor [9]. The leakage flux of the supporting bridges can also be reduced by using the bistate soft magnetic material, which can be treated nonmagnetically by heating [10], [11]. Therefore, the large supporting bridges are nonmagnetic. However, the bistate material is more expensive and has much smaller permeability than silicon steel used commonly with electric machines. In this paper, the electrical steel material is silicon steel for grade M400-50A.

In addition, a surface-inset permanent magnet rotor with structurally locked magnets is developed [12]. However, an electrically similar machine could be produced also with the buried magnets and the thin bridges around the magnets, where the bridges retain the magnets [6], [13]. Retainer bands and rings around the rotor are also commonly used with high-speed applications for rotors with the buried magnets [9] and with the surface magnets [6]. In addition, for very high speeds, a solid permanent magnet rotor with a slotless winding structure is also considered [14].

Contradictions between electrical and mechanical properties of the rotor were studied with many design processes [5], [6], [9]. However, optimizing procedures of the rotor structures with the interior permanent magnets is often done only electrically [15].

The magnets can also be used to support the rotor pole structure with the buried magnets. It can be done with the thinner supporting bridges [16] or without the supporting bridges [17], [18].

Manuscript received December 30, 2008; revised July 21, 2009. First published August 21, 2009; current version published December 11, 2009. This work was supported in part by ABB Oy, Motors, Finland.

The author is with ABB Oy, Motors, 65100 Vaasa, Finland (e-mail: jere.kolehmainen@fi.abb.com).

Digital Object Identifier 10.1109/TIE.2009.2029590

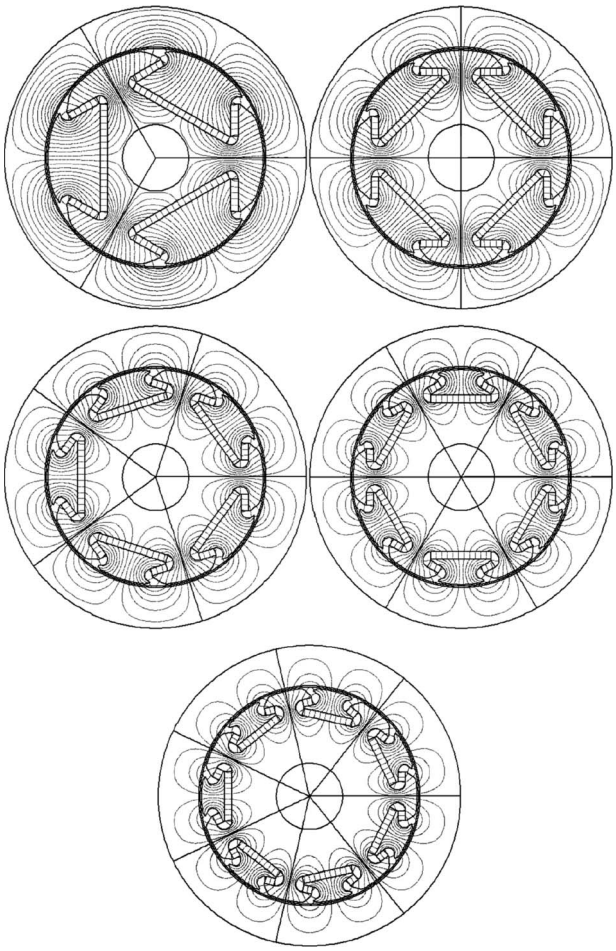

Fig. 1. Analyzed 6- to 14-pole rotor structures with flux lines.

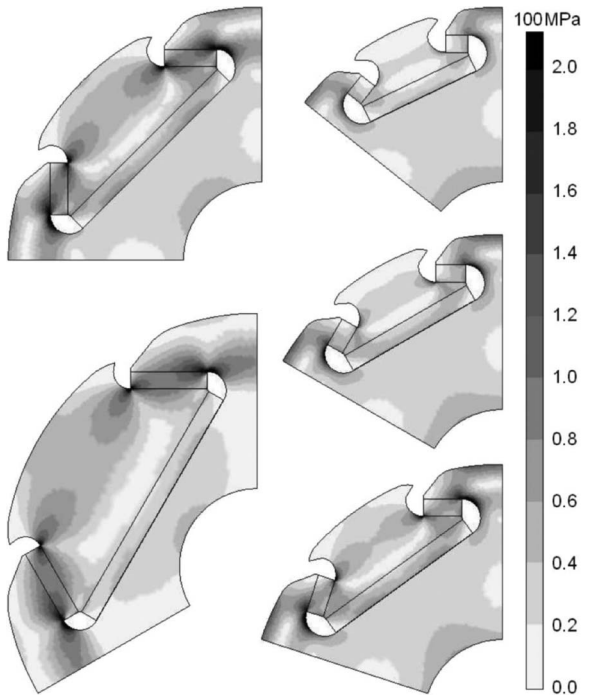

Fig. 2. von Mises stresses of two rotor poles in the analyzed 6- to 14-pole rotor structures.

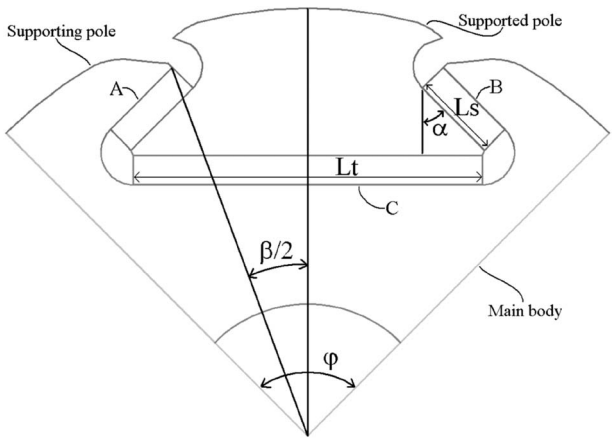

Fig. 3. Principle of the dovetail structure with parameters. Supporting magnets are marked as A and B. Tangential magnet is marked as C.

In these solutions, no extra supporting components are needed. In the dovetail-shaped poles without the supporting bridges, the tensile stress is geometrically converted into compressive one and only the magnets are used to support the pole structure. In this paper, the solution without the supporting bridges is studied. Rotor solutions with the various pole numbers of six to 14 are designed, optimized and compared. The optimizing procedures and comparisons are done with structural and electromagnetic analysis with the finite element method (FEM) [19], [20].

In addition, the practical solutions usually have so many electrical and structural possibilities, that before the optimizing process, many simplifications and choices for initial values have to be done, as it is done in this paper. Optimized solutions are also compared to three manufactured prototypes with the dovetail-shaped rotor poles.

II. Dovetail Rotors

The main principle of the dovetail rotor design in this paper is that every second pole of the rotor is mainly supported by the main body of the rotor through the magnets. The principle of the structure is shown in Figs. 1–3. The main body is first fitted to the shaft, and it contains every second pole of the rotor. The main body supports the rest of the alternating second poles through the pairs of the supporting magnets A and B. The shorter supporting magnets are located closer the air gap. The longer tangential magnets C, which are not supporting the structure, are located closer the shaft. The supported poles are separated from the supporting poles that belong to the main body. It also can be seen that rotor has the same number of symmetry sectors as pole pairs.

Pole separation increases electrical performance of the machine and dovetail-shaped poles lock the structure. Therefore, the structure is robust against centrifugal forces without losing significantly its electrical properties. In addition, no extra supporting devices are needed.

However, the dovetail machine has asymmetric poles. This decreases the maximum torque of dovetail machines, if the stator can see the asymmetric properties of the rotor. This also produces the homopolar flux to the rotor. Sometimes, it needs

to be decreased. In the tested three prototypes, there were no indications for problems caused by the homopolar flux. For example, the measured maximum flux density of 0.025 T in the shaft ends of the six-pole prototype motor is one indication of the homopolar flux.

The advantage of asymmetric poles is the possibility to decrease the torque and the current harmonics of the machines. Studies for decreasing the torque ripple by shifting pole pairs tangentially were done earlier [21], [22]. The torque ripple can also be reduced by changing stator properties and frequency conversion methods [23].

III. Initial Values for Optimizing

Dovetail rotors with six to 14 poles are designed by taking into account the electrical and the mechanical properties. The length and the diameter of the rotors are 250 and 292 mm. These are typical values for machine size IEC250. The rotor structures are designed by first choosing design criteria for getting robust structure against centrifugal forces and then optimizing it for finding the best electrical properties.

Obviously, the rotor structure becomes more robust with smaller supported pole mass, with larger supporting magnet area, and with better angle of the supporting magnets. However, with smaller supported pole mass, the supporting area of the magnets becomes smaller.

In addition to the rotor outer and the inner diameters and the length, more parameters are needed to be chosen to define rotor structures for all pole numbers. These parameters are the pole number, the radius and the angle (β in Fig. 3) of the outer points of the magnets, and the supporting angle (α in Fig. 3) of the supporting magnets. These properties define all other properties, for example, the position and the length (Ls in Fig. 3) of the tangential magnets, and the form of air gap between the poles. Some of the parameters can be chosen to be the same for all pole numbers.

Outer corners of the supporting magnets are chosen to have the same radius for all pole numbers.

For the mechanical strength point of view, theoretically, the best supporting angle of the supporting magnets α would be parallel with the air-gap surfaces in the middle of the supported poles. Then, $\alpha = 90^\circ$. However, with the best theoretical angle, the electrical and other strength properties become worse. In addition, practical solution is difficult to find. The supporting angle α is optimized with some cases. The best supporting angles are the same angles as the rotor surface in the middle of supporting poles. In other words, the two supporting magnets A and B of one supporting pole are parallel with each other. Then, $\alpha = 90^\circ - \varphi/2$, where φ is the angle of the pole pairs. Therefore, the chosen supporting angles are used in the final optimizing process.

A preliminary electrical optimizing process, where average air-gap flux densities are maximized, shows that of all pole numbers the best outer point angles β of the supporting magnets A and B of one supported pole are near 90% of average angle of the poles as $\beta = 0.9\varphi$. The supported poles are tangentially smaller than the supporting poles. With the smaller supported pole angle of $\beta < 0.9\varphi$, there can also be more magnetic material and the air-gap flux becomes larger. However, a smaller supported pole angle also increases the leakage flux between the poles near the air gap, which decreases the air-gap flux. Effects of asymmetry to the air-gap flux density distribution are eliminated with the structure near the air gap. The angle of the outer points of the supporting magnets of 90% of the average angle of the poles of $\beta = 0.9\varphi$ is chosen to be used in later studies.

With the chosen structure properties, the length of the supporting magnets A and B defines positions and lengths of the longer tangential magnets C. In the following optimizing process, effects of changing length of the supporting magnets are studied to strengthen electrical properties of the dovetail-shaped rotors. The designs for six to 14 poles can be seen with flux lines and stress distributions in Figs. 1 and 2.

IV. Mechanical Strength Definition Method

For the dovetail-shaped rotor design, the strength of the rotor is important to define to find an optimal solution. In this paper, the mechanical FEM [19] with some heuristic calculation rules are used.

Maximum speed of the rotor is defined from von Mises stresses at a speed of 6000 1/min with the equation

$$n_{\max} = n_{\text{calc}} \cdot \sqrt{\sigma_{\text{yield}}/(R_{\text{calc}} \cdot \eta)} \tag{1}$$

where $n_{\max}$, n_{calc}, η, σ_{yield}, and R_{calc} are maximum speed, calculation speed, factor of safety, yield strength, and calculated critical stress, respectively.

Critical von Mises stresses of the magnets are assumed to be in the middle of the magnets, even though the maximum stress points in the calculations are in the corners of the magnets. However, exact critical points of stress are impossible to define, because of possible filling material, sliding, and roughness between the magnets and rotor stack affect to stress distribution in the surfaces of the magnets. In addition, brittleness of the magnetic material might cause unpredictable effects.

For the used magnetic material Nd–Fe–B, the typical tensile strength is 70 MPa and the flexural strength is 240 MPa. The used Young's modulus is 150 GPa for magnetic material while it is 205 GPa for electric sheet material. In the electrical calculations, the Nd–Fe–B has the remanence flux density 1.03 T and the coercive field 780 kA/m.

In this paper, the allowed maximum stress of the magnets is chosen to be tensile strength 70 MPa with the safety factor 1.5 in spite of higher flexural strength. For electric sheets, the tensile strength 300 MPa was chosen to be the allowed maximum stress also with the safety factor 1.5.

In the all-modeled structures, the strength of the electric sheet stack comes important only with the longest supporting magnets and with the thin radial parts of the rotor body. For smaller lengths of the supporting magnets, the strength of the supporting magnets is critical for the durability of the rotors. Therefore, the speed durability of the supporting magnets could be used to define the speed durability of the whole designed machine with almost all lengths of the supporting magnets.

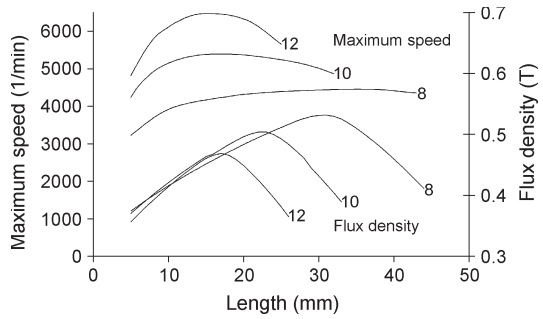

Fig. 4. (Upper curves) Maximum speeds of the rotors and (lower curves) average flux densities in air gaps as a function of supporting magnet length Ls in 8- to 12-pole rotor structures.

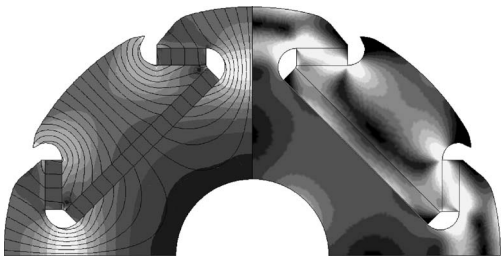

Fig. 5. (Left) Flux densities and lines (right) and von Mises stresses of two rotor poles in the eight-pole rotor structure. Highest values are colored with lightest colors.

V. Optimizing Process

The dovetail designs with chosen criteria are studied from electrical and strength points of view. The ideal parameter values are searched for. The average flux density in the air gap and the maximum speed are used as optimizing goals.

First, maximum speeds of all possible solutions are defined. Therefore, von Mises stresses at a speed of 6000 1/min are calculated for the rotor with the different pole numbers and the lengths Ls of the supporting magnets. The maximum speeds of the rotors with the each pole number and with the large length scale of the supporting magnets are defined from these calculations with the method defined earlier. The resulted maximum speeds of the rotors with different pole numbers have relatively slight maxima as shown in Fig. 4.

The flux densities in the air gap are also calculated with the same structures as a function of supporting magnet length Ls. The comparison between the maximum speeds and the average flux densities in the air gaps of 8- to 12-pole machines is also shown in Fig. 4. The air-gap flux has clearly sharper maxima with all the shown pole numbers, than the maximum speed. In addition, when the average flux densities in the air gaps are largest, the machines have also almost strongest mechanical structures with all pole numbers.

In the cross sections of the rotors, electrically and structurally critical areas are near each other as shown in Fig. 5. For example, when the necks of the supporting poles are decreasing, both the strength and magnetic conductivity of the necks are increasing.

For defining the optimal solution, the average flux densities in the air gaps as a function of the total mass of the magnets are shown in Fig. 6. There are clear maxima in the flux densities.

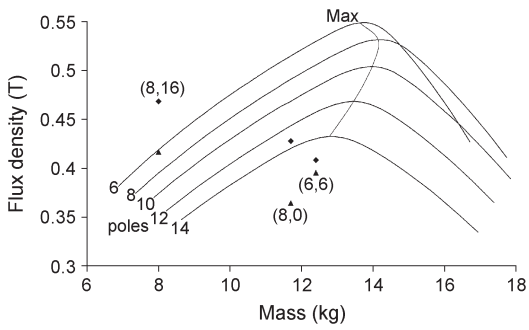

Fig. 6. Average flux densities in the air gap as a function of total mass of the magnets in 6- to 14-pole rotor structures. Measured and analyzed prototype values are marked as triangles and diamonds and (poles, bridges).

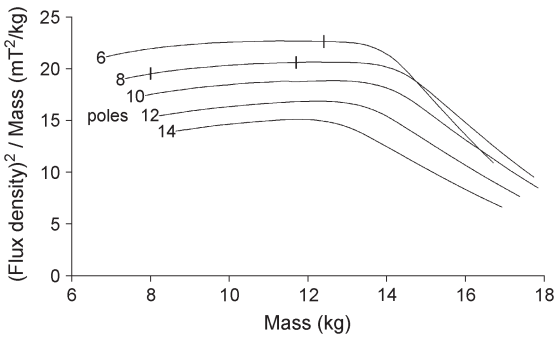

Fig. 7. Square of average flux densities in air gaps over masses as a function of total mass of magnets in 6- to 14-pole rotor structures. Masses of magnets in the prototypes are marked with vertical lines.

Below the maxima, the flux densities are increasing almost proportionally with the total masses of the magnets. Hence, the ratios of the flux and the masses of the magnets are in the acceptable level. This ratio should always be near its maxima. Otherwise, a part of the magnetic material is wasted and the rotor is saturated. After flux density maxima, flux densities are decreasing because of saturation in the radial bridges of the rotor bodies.

The best structures are obtained with the smaller lengths of the supporting magnets Ls before saturation effect, because then the efficiency of magnetic material remains good and the largest amount of magnets can be inserted to the rotor. However, in real machines with the supplied voltage, the saturation effect could appear with the smaller masses of the magnets and the best structure could be different. In addition, the largest possible amount of magnetic material is not always the best solution.

For studying further the electric quality of the structures, the effects of the masses of the magnets to the maximum torque are shown in Fig. 7 as a function of square of the average flux density in the air gaps over the mass of the magnets. This is based on the fact that the maximum torque of the electric machine is proportional to square of the air-gap flux. The values increase slightly almost up to the saturation areas. This implies that the best ratio of the maximum torque and the mass of the magnet for the different pole numbers are near the saturation area.

The optimal design can be chosen using many criteria. For higher pole numbers, the maximum speeds of the machines are higher and expected maximum torques with the same amount of

TABLE I
PROPERTIES OF DESIGNED ROTORS

Pole number	Total mass of magnets (kg)	Average flux density in air gap (T)	Maximum speed (1/min)
6	13.4	0.547	4350
8	13.7	0.529	4380
10	13.5	0.494	5300
12	13.1	0.462	6470
14	12.5	0.426	7750

the magnets is smaller. The largest expected maximum torque can be reached with higher masses of the magnets than the best ratios of the maximum torque and the mass of the magnets.

VI. Optimized Designs

The average magnitudes of the flux densities in the air gaps are maximized by finding ideal tangential positions β and lengths Ls of the supporting magnets. The resulting rotor structures with flux lines are shown in Fig. 1. The average magnitudes of the flux densities in the air gaps, and masses of the magnets are shown in Table I. The average flux density is the total flux of the outer surface of the air gap divided by its area.

The resulted total masses of the magnets with the all pole numbers are near each other. However, the average maximum flux density decreases with the higher pole numbers. There are more routes for the leakage flux with the higher pole numbers, and the average air-gap flux density is expected to be lower with the same amount of magnet material.

For optimized designs with all pole numbers, von Mises stresses at a speed 6000 1/min are shown in Fig. 2. Higher stresses are shown with darker colors and the scale is 0 to 200 MPa. The maximum allowed speed for the resulting designs defined from the stress calculations are shown in Table I.

It can be seen that the stresses are lower for the higher pole numbers. Therefore, rotors with higher pole numbers are stronger compared to rotors with lower pole numbers. Otherwise, the total air-gap flux is smaller with a higher pole number as it is expected. In addition, the electrical properties of the rotors are better for lower pole numbers. However, worsening the electrical properties by increasing the pole number increases the rotor strength substantially.

In the real solution, there should be shaft in the rotor. Sometimes, the size of the area inside the pole's structure could be critical in the machine solutions. In the dovetail solutions considered in this paper, there is more space on the shaft side, increasing with the pole number. This can be valuable in some applications as, for example, machines with hollow shaft or cooling channels. The maximum shaft sizes are estimated to be of the same radius than the flux density is 0.2 T in the middle of the supporting poles in the present calculations. With this estimation, the effect of shaft is still practically negligible to the electrical properties. In addition, with this estimation, the structural properties remain also practically unchanged. The maxima of the shaft radiuses are shown in Table II. For comparison to the other solutions than the dovetail-shaped pole, the maximum shaft sizes are also estimated for electrically similar rotors with the radial magnets by calculating the distances between the

TABLE II
MAXIMUM SHAFT SIZES

Pole number	Maximum radius with dovetail design (mm)	Maximum radius with radial magnets (mm)
6	50	17
8	60	43
10	69	62
12	77	76
14	82	87

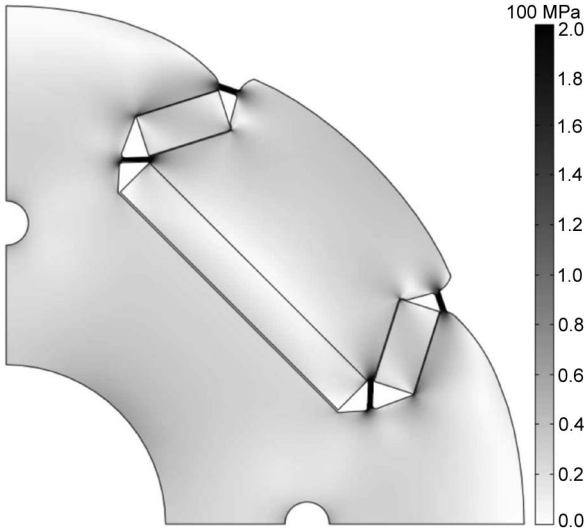

Fig. 8. von Mises stresses of two rotor poles in the manufactured eight-pole rotor structures with bridges between poles.

radial magnets and the middle of the rotor in Table II. However, for the radial magnets solution, the allowed shaft sizes are smaller and also some extra supporting structures. Hence, the dovetail design allows more space to the shaft side than the radial magnet design.

In addition, in the real solutions with higher pole numbers, higher supply frequencies are needed. This is also worse for electrical properties of the dovetail machines with high pole numbers compared to low pole numbers. In conclusion, the dovetail rotors with higher pole number are stronger against centrifugal forces and with lower pole number, they are electrically better.

VII. Comparison of Prototypes

Three prototypes with the dovetail-shaped poles are designed separately with the optimization method of this paper [16], [17], [18]. Optimal solutions are found with the modeling and improvement method. In this method, dimensions and positions of the magnets are separately changed and then electrical and mechanical properties of the machines are modeled (see Figs. 8–10). Designs with best electrical results with strong enough rotors are chosen. These prototypes are compared with the optimized designs.

First, two eight-pole prototypes [16], [17], [18], with the same rotor dimensions as that with the optimized design, are produced (see Figs. 8, 9, 11 and 12). Then, one smaller six-pole prototype is manufactured (see Figs. 10 and 13). The length and the diameter of the smaller six-pole prototype rotor are 165 and

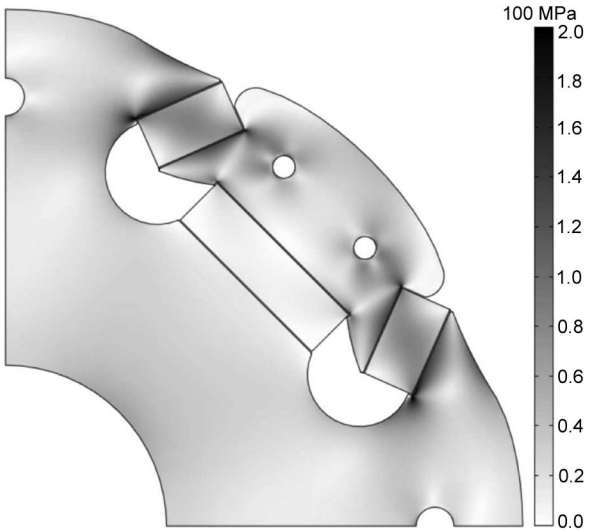

Fig. 9. von Mises stresses of two rotor poles in the manufactured eight-pole rotor structures without bridges between poles.

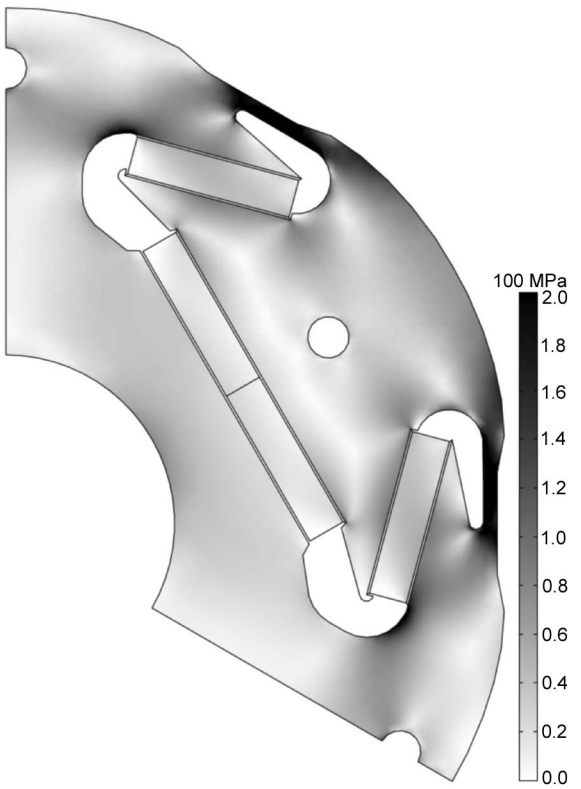

Fig. 10. von Mises stresses of two rotor poles in the manufactured six-pole rotor structure with bridges between poles.

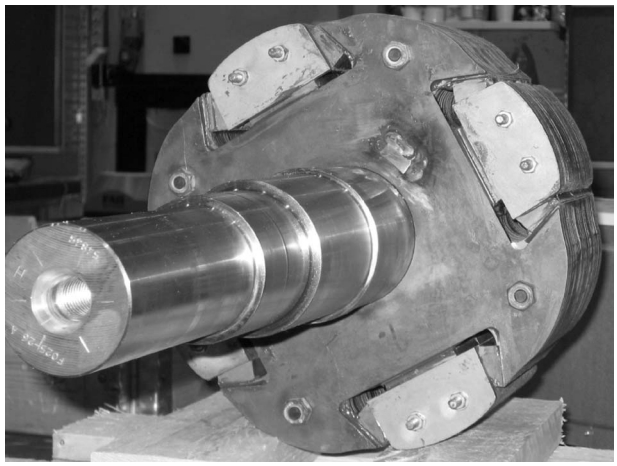

Fig. 11. Prototype of eight-pole rotor without bridges.

Fig. 12. Prototype of eight-pole rotor with bridges.

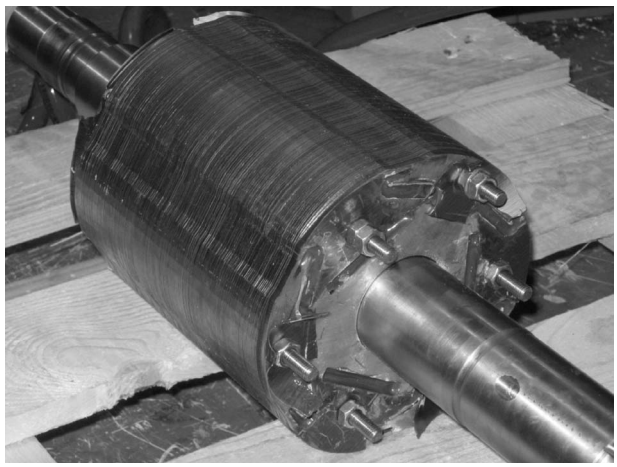

Fig. 13. Prototype of six-pole rotor with bridges.

165 mm, respectively. In this paper, all the shown results are scaled to the dimensions of the other considered designs and marked with $(^*)$. The scaling of the size is done with the factor as 292 mm/165 mm. The power and the maximum speed are also scaled with the help of the factor.

The manufacturing method of the two rotors with the solid rotor plates with the bridges between the poles (see Figs. 12 and 13) was to assemble a stack of disks, compress it using bolts and nonmagnetic end plates and shrink fit the stack on the shaft. Then, the magnets are inserted into their holes using glue. The rotor with the separate alternating rotor poles without the bridges between the poles (see Fig. 11) is manufactured with a different method, which is to assemble five (one main body and four small poles) stacks of disks, compress them using bolts and nonmagnetic end plates and shrink fit the main body stack on the shaft. Next, the magnets are fixed to four-pole stacks using

TABLE III
PROPERTIES OF PROTOTYPES

Poles, Bridges	Total mass of magnets (kg)	Maximum speed without bridges (1/min)	Maximum speed (1/min)
6, 6	12.4	4243	5651
8, 16	8.0	4264	4997
8, 0	11.7	4602	4602

TABLE IV
TEST VALUES

Poles, Bridges	Nominal Power (kW)	Load test speed (1/min)	Maximum speed (1/min)
6, 6	122*	4487*	4487*
8, 16	185	4000	5500
8, 0	110	4800	4800

glue. Resulting poles are axially inserted to main body stack using glue.

In the real rotor solutions, some modifications have to be introduced for the optimized ideal solutions. The air-gap thickness is varying between the different motor solutions. The thickness of the air gap is wanted to be larger between the poles than in the middles of poles. In addition, needed effective magnetic thicknesses and the lengths of the magnets are usually different and affect to a resulted solution. In the real designs, large area, where the ratio of the air-gap flux and the mass of magnets is good and the saturation level of the rotor is low, are usable. The masses of the magnets in the prototypes are marked to Fig. 7 with vertical lines.

The eight-pole prototypes have smaller supporting angles of the supporting magnets than the designs optimized earlier. Conversely, the six-pole prototype has larger supporting angles of the supporting magnets than the designs optimized earlier. In the two prototypes, the tangential magnets are also shorter than the distance between inner corners of the supporting magnets. Therefore, some extra structure is created. These changes to optimal design are needed for saving magnetic material. However, relative saving of magnetic material compared to the designs optimized earlier are -7.1%, -41.4%, and -14.3% for the six-pole machine, the eight-pole machine with the bridges and the eight-pole machine without the bridges, respectively.

Although there are also some bridges between the poles in the two designs, strength analysis of the prototypes is also done without the bridges. The analyzed maximum speeds are shown in Table III. The maximum speeds without the bridges are defined with the same method as with the optimized ideal solutions considered earlier. With the bridges, the machines have higher maximum speeds. In the solution with the bridges, the critical von Mises stresses for maximum speed are in the bridges. However, the bridges support partly the structure and make the rotor stronger.

The three prototype motors are manufactured with commonly used stator for the three phase winding. Tests are done with the frequency converters and the load machines.

All machines are driven for at least one heat test with the nominal loads and the output powers (see Table IV). All machines were stable through tests, as expected. There were no indications of deformation during the tests. The six-pole motor values are scaled to the considered machines size $(^*)$.

TABLE V
AVERAGE FLUX DENSITIES IN AIR GAPS (IN TESLA)

Poles, Bridges	Corresponding optimized	Analyzed prototypes	Measured prototypes
6, 6	0.547	0.408	0.396
8, 16	0.529	0.468	0.417
8, 0	0.529	0.428	0.364

Average air-gap flux densities in the air gap B_{airgap} are compared in Table V. The average air-gap flux densities of the prototypes produced only by the rotors are estimated from the open-circuit voltages U_{oc} with the equation

$$B_{\mathrm{airgap}} = U_{\mathrm{oc}} \Big/ \left(\omega N \frac{2}{\pi} \tau L\right) \tag{2}$$

where ω, N, τ, and L are the electrical angular speed, the number of turns, the pole pitch, and the axial length of the rotor, respectively [24]. Sinusoidal assumption included to the equation gives good results, because the open-circuit voltages and air-gap flux densities are near sinusoidal in the prototype motors. The measured flux densities of the prototypes are from 3% to 15% smaller than the analyzed ones. Corresponding optimized values are larger than the values of the prototypes, because of smaller relative amount of magnetic material of the prototypes (see Fig. 5). In addition, the measured and analyzed ratios of the air-gap flux density and the mass of the magnets are smaller in the six-pole prototype and in the eight-pole prototype without the bridges than optimized values. Conversely, this ratio is larger in the eight-pole prototype with the bridges, because of the smaller relative air gap. However, these ratios of the prototypes are near with the optimized ones.

The optimizing process is reasonable when comparing it to the real design. The main properties of the behavior of the dovetail-shaped rotor design have been found.

VIII. CONCLUSION

Many design aspects of the dovetail-shaped rotor structure have been found by using simplified electromagnetic and strength models. The optimal shapes of the poles are searched and discussed. The effects of the pole number to electrical and mechanical properties of the dovetail machine were determined.

It is shown that the total air-gap flux is decreasing and the maximum allowed speed is remarkably increasing when increasing the pole number. Although the study is done with the optimized rotor structures with the pole numbers six to 14, it can be used as a general rule for choosing the pole number of the machines for different solutions. Therefore, the rule can be stated as follows: Increasing the strength of the rotor by increasing the pole number decreases the electrical performance.

In addition, the dovetail-shaped rotor structures with six to 14 poles is shown to exhibit a significant increase in mechanical stability over the conventional bridge fixed pole design.

Finally, the results with the three prototype motors, designed and optimized separately with this study, show feasibility of the dovetail-shaped rotor structure and the optimized results.

According to this paper, the dovetail rotor machines with higher pole number are stronger and with lower pole number electrically better.

ACKNOWLEDGMENT

The author would like to thank J. Ikäheimo of ABB Oy, Motors, for his support and collaboration.

REFERENCES

[1] A. Piippo, M. Hinkkanen, and J. Luomi, "Analysis of an adaptive observer for sensorless control of interior permanent magnet synchronous motors," *IEEE Trans. Ind. Electron.*, vol. 55, no. 2, pp. 570–576, Feb. 2008.

[2] B. K. Bose, "A high-performance inverter-fed drive system of an interior permanent magnet synchronous machine," *IEEE Trans. Ind. Appl.*, vol. 24, no. 6, pp. 987–997, Nov. 1988.

[3] S. Morimoto, M. Sanada, and Y. Takeda, "Inverter-driven synchronous motors for constant power," *IEEE Ind. Appl. Mag.*, vol. 2, no. 6, pp. 18–24, Nov./Dec. 1996.

[4] K. J. Tseng and S. B. Wee, "Analysis of flux distribution and core losses in interior permanent magnet motor," *IEEE Trans. Energy Convers.*, vol. 14, no. 4, pp. 969–975, Dec. 1999.

[5] R. Dutta and M. F. Rahman, "Design and analysis of an interior permanent magnet machine with very wide constant power operation range," *IEEE Trans. Energy Convers.*, vol. 23, no. 1, pp. 25–33, Mar. 2008.

[6] A. Binder, T. Schneider, and M. Klohr, "Fixation of buried and surface mounted magnets in high-speed permanent-magnet synchronous machines," *IEEE Trans. Ind. Appl.*, vol. 42, no. 4, pp. 1031–1037, Jul./Aug. 2006.

[7] F. Morel, J.-M. Retif, L.-S. Xuefang, and C. Valentin, "Permanent magnet synchronous machine hybrid torque control," *IEEE Trans. Ind. Electron.*, vol. 55, no. 2, pp. 501–511, Feb. 2008.

[8] H. Jin and J. Lee, "An RMRAC current regulator for permanent-magnet synchronous motor based on statistical model interpretation," *IEEE Trans. Ind. Electron.*, vol. 56, no. 1, pp. 169–177, Jan. 2009.

[9] E. C. Lovelace, T. M. Jahns, T. A. Keim, and J. H. Lang, "Mechanical design considerations for conventionally laminated, high speed, interior PM synchronous machine rotors," *IEEE Trans. Ind. Appl.*, vol. 40, no. 3, pp. 806–812, May/Jun. 2004.

[10] A. M. El-Refaie, R. Manzke, and T. M. Jahns, "Application of Bi-state magnetic material to automotive offset-coupled IPM starter/alternator machine," *IEEE Trans. Ind. Appl.*, vol. 40, no. 3, pp. 717–725, May/Jun. 2004.

[11] A. M. El-Refaie and T. M. Jahns, "Application of Bi-state magnetic material to an automotive IPM starter/alternator machine," *IEEE Trans. Energy Convers.*, vol. 20, no. 1, pp. 71–79, Mar. 2005.

[12] J. Gan, K. T. Chau, C. C. Chan, and J. Z. Jiang, "A new surface-inset, permanents-magnet, brushless dc motor drive for electric vehicles," *IEEE Trans. Magn.*, vol. 36, no. 5, pp. 3810–3818, Sep. 2000.

[13] M. W. Degner, R. van Maaren, A. Fahim, D. W. Novotny, R. D. Lorenz, and C. D. Syverson, "A rotor lamination design for surface magnet retention at high speeds," *IEEE Trans. Ind. Appl.*, vol. 32, no. 2, pp. 380–385, Mar./Apr. 1996.

[14] C. Zwyssig, S. D. Round, and J. W. Kolar, "An ultrahigh-speed, low power electrical drive system," *IEEE Trans. Ind. Electron.*, vol. 55, no. 2, pp. 577–585, Feb. 2008.

[15] T. Ohnishi and N. Takahashi, "Optimal design of efficient IPM motor using finite element method," *IEEE Trans. Magn.*, vol. 36, no. 5, pp. 3537–3539, Sep. 2000.

[16] J. Kolehmainen and J. Ikäheimo, "Motors with buried magnets for medium speed applications," *IEEE Trans. Energy Convers.*, vol. 23, no. 1, pp. 86–91, Mar. 2008.

[17] J. Kolehmainen, "Machine with a rotor structure supported only by buried magnets," in *Proc. ISEF*, Prague, Czech Republic, Sep. 2007. CD-ROM, Paper 023.

[18] S. Wiak, A. Krawczyk, and I. Dolezel, Eds., *Advanced Computer Techniques in Applied Electromagnetics*, vol. 30, *Studies in Applied Electromagnetics and Mechanics*. Amsterdam, The Netherlands: IOS Press, 2008, pp. 240–246.

[19] *COMSOL Multiphysics Software*, 2009. [Online]. Available: www.comsol.com

[20] *FLUX Software*, 2009. [Online]. Available: www.cedrat-groupe.com

[21] T. Ishikawa and G. Slemon, "A method of reducing ripple torque in permanent magnet motors without skewing," *IEEE Trans. Magn.*, vol. 29, no. 2, pp. 2028–2031, Mar. 1993.

[22] T. Li and G. Slemon, "Reduction of cogging torque in permanent magnet motors," *IEEE Trans. Magn.*, vol. 24, no. 6, pp. 2901–2903, Nov. 1998.

[23] L. Parsa and L. Hao, "Interior permanent magnet motors with reduced torque pulsation," *IEEE Trans. Ind. Electron.*, vol. 55, no. 2, pp. 602–609, Feb. 2008.

[24] J. F. Gieras and M. Wing, *Permanent Magnet Motor Technology—Design and Applications*., 2nd ed. New York: Marcel Dekker, 2002, pp. 381–383.

[25] J. Kolehmainen, "Dovetail permanent magnet rotor solutions with different pole numbers," in *Proc. ICEM*, Vilamoura, Portugal, Sep. 2008, pp. 1–4.

Jere Kolehmainen received the M.Sc. and Ph.D. degrees in theoretical physics from the University of Jyväskylä, Jyväskylä, Finland, in 1996 and 2000, respectively.

He is currently with ABB Oy, Motors, Vaasa, Finland. He is interested in synchronous and induction ac machines and electromagnetic modeling.